An optical chopper based re-circulating loop for few-mode fiber transmission

V.A.J.M. Sleiffer,[1,*] Y. Jung,[2] M. Kuschnerov,[3] S. U. Alam,[2] D. J. Richardson,[2] L. Grüner-Nielsen,[4] Y. Sun,[5] and H. de Waardt[1]

[1]*COBRA institute, Eindhoven University of Technology, Den Dolech 2, 5612AZ, Eindhoven, The Netherlands*
[2]*Optoelectronics Research Centre, University of Southampton, Highfield, Southampton, Hampshire, SO17 1BJ, UK*
[3]*Coriant R&D GmbH, St. Martin-Str. 76, 81541 Munich, Germany*
[4]*OFS, Priorparken 680, 2605 Brøndby, Denmark*
[5]*OFS, 2000 Northeast Expressway, Norcross, GA 30071, US*
**Corresponding author: v.a.j.m.sleiffer@tue.nl*

An optical chopper based re-circulating loop is presented for emulating long-haul transmission using few-mode fiber. A proper functioning of the loop is verified by transmission of 3 mode-division multiplexed × 128-Gb/s DP-QPSK over more than 1000 km of few-mode fiber.

For the past ~30 years single-mode fiber (SMF) has served our planet as long-haul transmission medium of choice due to its low-loss over a large bandwidth, offering a huge data capacity within just a single fiber [1, 2]. To investigate long-haul transmission in the laboratory it is impractical to have the large number of fiber spools and erbium-doped fiber amplifiers (EDFAs) required for a straight-line embodiment of a long-haul transmission line, and therefore re-circulating loops containing up to several hundred kilometers of fiber are used to emulate long-haul distances [3, 4].

Research over the last years has shown that current deployed single-mode fiber (SMF) systems will reach their capacity limits within the next decade or so, since data traffic is growing exponentially and the Kerr effect (fiber nonlinearity) is putting a limit on the maximum spectral efficiency achievable over a certain transmission distance [5]. This means new fibers will have to be deployed sooner or later. Anticipating this future need there is consequently great interest in developing more cost-effective means to accommodate the future growth data demands than simply deploying a large number of parallel SMF links. Space-division multiplexing (SDM) [6, 7], which targets an increase in the capacity of a single fiber by using multiple modes and/or cores, is currently being vigorously pursued as a potential solution.

Whilst the first steps in SDM research were mainly directed towards proving technological feasibility, the critical next step is to demonstrate that the various approaches under investigation are able to support long distance transmission, which is after all the main driver behind SDM technology. To be able to do this in a lab environment, a re-circulating loop has to be realized.

The first approaches to such re-circulating loops for few-mode fiber (FMF) systems were based on the previous single-mode technology [8, 9], incorporating a number of single-mode $LiNbO_3$ switches (one for each mode supported by the FMF) for opening and closing the loop in the single-mode domain (since few-mode fiber switches are not available at present) and an identical number of EDFAs (since these experiments did not use a few-mode (FM)-EDFA) which requires de-multiplexing the modes every circulation of the loop [10, 11].

In [12] the first all-FMF re-circulating loop, with a FM-EDFA, was presented where a mechanical free-space loop switch was employed. In [13] we also showed an all-FMF re-circulating loop, based on an optical chopper to do the switching of the loop, but without details on the operation of the loop. In this letter we present in more detail the operation of such a loop, with verification of proper functioning by showing transmission results of a 3 mode-division multiplexed (MDM) × 128-Gb/s DP-QPSK over a more than 1000 km long transmission distance.

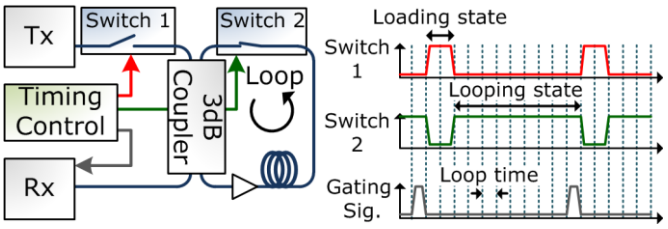

Fig. 1. Schematic setup of a SMF re-circulating loop.

The operation of a SMF re-circulating loop is described in [8, 9] and depicted in Fig. 1. In the first step the loop is completely filled with light signal by closing the switch 1 to the transmitter and opening the loop switch 2, called the loading state, for a duration longer than the loop time (the roundtrip time delay for the optical signal to travel through the loop). The loop time for a $L = 60 \cdot 10^3$m loop, as used in the experiment described later, is calculated in

equation (1) assuming a refractive group index of $n_g \approx 1.45$ and the speed of light $c \approx 3 \cdot 10^8$ m/s.

$$\tau_{loop} = \frac{n_g \cdot L}{c} = \frac{1.45 \cdot 60 \cdot 10^3}{3 \cdot 10^8} = 290 \mu s \qquad (1)$$

The next state is the looping state, i.e. closing the loop switch 2 and blocking further signal from transmitter. This allows the trapped light signal to circulate around the loop (which incorporates EDFAs). The length of this state defines the emulated transmission distance, i.e. the total number of loops. By triggering (gating) the receiver, which is receiving light continuously, at the right time the signal can be analysed after a certain transmission distance. By choosing the gating signal to be shorter than the loop time, burst errors at the edges of the time window are avoided, which occur due to the rise and fall times of the loop switch. In SMF re-circulating loops the switching is usually performed by acousto-optic modulators (AOMs), or fast electro-optic switches like $LiNbO_3$ switches.

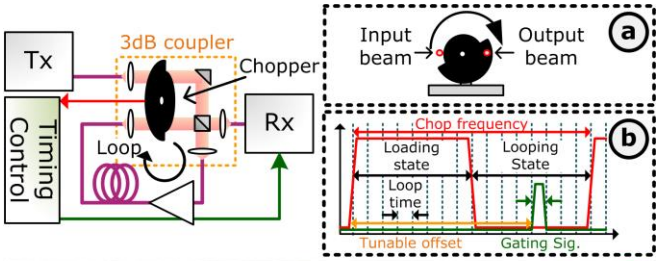

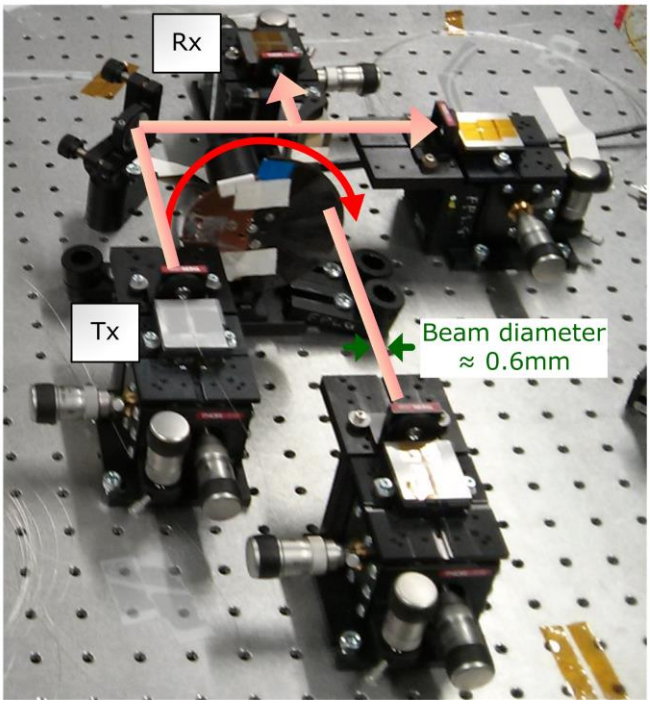

Fig. 2. Optical chopper re-circulating loop, a) beam positioning and b) timing control

The same switching operation can however be obtained by using an optical chopper within a free-space 3dB coupler and some control signals, as depicted in Fig. 2. This approach gives great flexibility; every kind of FMF can be used in principle. Moreover lossy switches are avoided. In this particular case a single-slot chopper blade is used, but in principle a multi-slot blade can be used if the following conditions are satisfied. By using optical stages, the signal beam coming from the transmitter (input beam) is positioned in the same plane as the loop-output beam (output beam), to make sure that when the chopper is blocking the input beam the output beam is not blocked and vice versa (Fig. 2a).

The rise and fall time of the switching are determined by the chop frequency, beam size and the position of the beams with respect to the center of the blade. In the experiment a blade with a diameter of 4 inch ≈ 101.6 mm was used, and set to run at a chop frequency of $f = 50$ Hz. The beams were positioned at the outside of the blade ($r_{blade} = 5 \cdot 10^{-2}$m) to obtain the fastest rise and fall times, having a rotational speed at that position of:

$$v_{rot} = 2 \cdot \pi \cdot r_{blade} \cdot f = 2 \cdot \pi \cdot 5 \cdot 10^{-2} \cdot 50 \approx 15.7 \frac{m}{s} \qquad (2)$$

The choice of lenses influences the fiber-to-fiber coupling loss and the mode-dependent loss (MDL), as well as the collimated beam diameter obtained inside the free-space 3dB coupler. Lenses with a focal length of 4.51 mm were used in the experiment, achieving low coupling loss (<2 dB) and MDL (<0.5 dB), and resulting in a measured collimated beam diameter of around 0.6 mm. This yields, approximating the diameter as being the distance to be covered by the blade, a rise and fall time of $0.6 \cdot 10^{-3}/15.7 \approx 40$ µs. The measurements of the rise and fall times, depicted in Fig. 3 agree well with this calculated time. This indicates that with a 60 km FMF-loop in the worst case, i.e. sequential closing the input beam and passing the output beam, enough signal is left for analysis ($290\text{-}2 \cdot 40 = 210$ µs) given that one million samples on the 50 GSamples/s digital sampling oscilloscope (DSO) and 80 thousand samples on the 40 GSamples/s scope are stored, which equals a time of 20 µs.

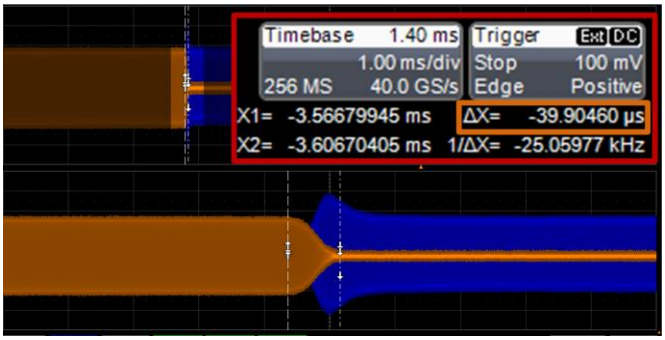

Fig. 3. Rise (blue) and fall (orange) time measurement of the optical chopper re-circulating loop (≈ 40 µs)

The chop frequency (and blade used) also defines the maximum number of loops that the signal can travel before the loop is re-loaded (Fig. 2b) which is equal to the looping state divided by the loop time. Note this is not the case for an AOM switched loop where the loop time is controlled electronically. To collect the signal in an optical chopper operated loop after a certain distance, the DSOs have to be triggered at the right time. To achieve this, the reference signal produced by the photodiode inside the chopper itself to control the chop frequency is fed to a timing-control box, which produces a trigger after a tunable offset time. By first determining

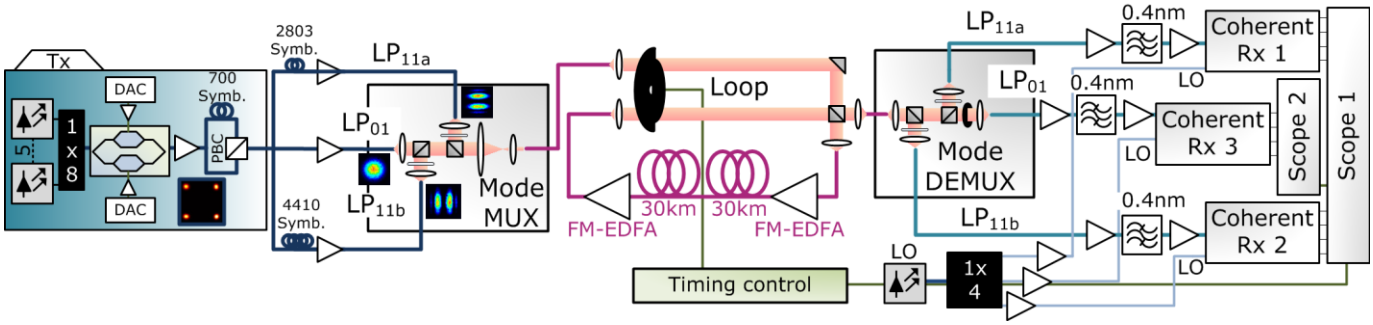

Fig. 4. Optical chopper re-circulating loop experimental setup for transmission of 3 MDM × 128 Gb/s DP-QPSK over FMF.

the static delay between the chopper reference signal and the actual signal appearing on the DSOs, the signal after a certain number of loops can be collected by setting the offset time to the static delay (first loop) plus the n times the additional loop time, to analyze the signal after n+1 loops.

Fig. 4 depicts the experimental setup using an optical chopper re-circulating loop to emulate transmission distance over FMF supporting the linearly-polarized LP_{01}, and LP_{11} modes [14]. At the transmitter side five lasers running at 193.0, 193.1, 193.4 (channel under test (CUT)), 193.8 and 193.9 THz were passively combined using a 1×8 polarization maintaining coupler, and subsequently modulated using an IQ-modulator, driven by two digital-to-analog converters running at a 32GBaud symbol rate with 1 sample/symbol that address the in-phase and quadrature ports of the IQ-modulator. The electrical driving signal was formed by combining two pseudo random binary sequences of length 2^{15} which were shifted by 16383 symbols with respect to each other before combining them and mapping them onto QPSK symbols.

After modulation, polarization-multiplexing was emulated by splitting the signal into two equally powered tributaries, delaying one by 700 symbols for de-correlation, and combining them again using a polarization beam combiner (PBC). The 128-Gb/s DP-QPSK signal subsequently is split into three signals which are delayed by 2803 and 4410 symbols with respect to the original signal again for emulation of three different signals, and fed to the phase-plate based mode multiplexer (MUX), more detailed described in [15], which launches the signals into a 3 mode supporting FMF-pigtail.

Tab. 1. 60 km FMF span (@ 1550nm)

	Spool 1	Spool 2
Length [km]	30	30
Distributed Mode Coupling [dB]	-26	-25
DGD [ps/m]	-0.044	0.053
Disp. LP_{01}/ LP_{11} [ps/(nm·km)]	19.8 / 20	19.8 / 20
Attenuation LP_{01}/ LP_{11} [dB/km]	0.198 / 0.191	0.198 / 0.191

The FMF pigtail was connected to the free-space 3dB coupler. The input signal was coupled into the loop containing two few-mode (FM) EDFAs [16], and 60 km of FMF with the parameters listed in Tab. 1. The 60 km FMF span has a differential group delay (DGD) between the LP_{01} and LP_{11} modes of around 9 symbols. At the input and output of the loop a FM-EDFA was placed to compensate for the span and coupling loss of the 3dB coupler. The MDL after one loop was measured to be ~0.5 dB. A low MDL is crucial to obtain a long transmission distance [12].

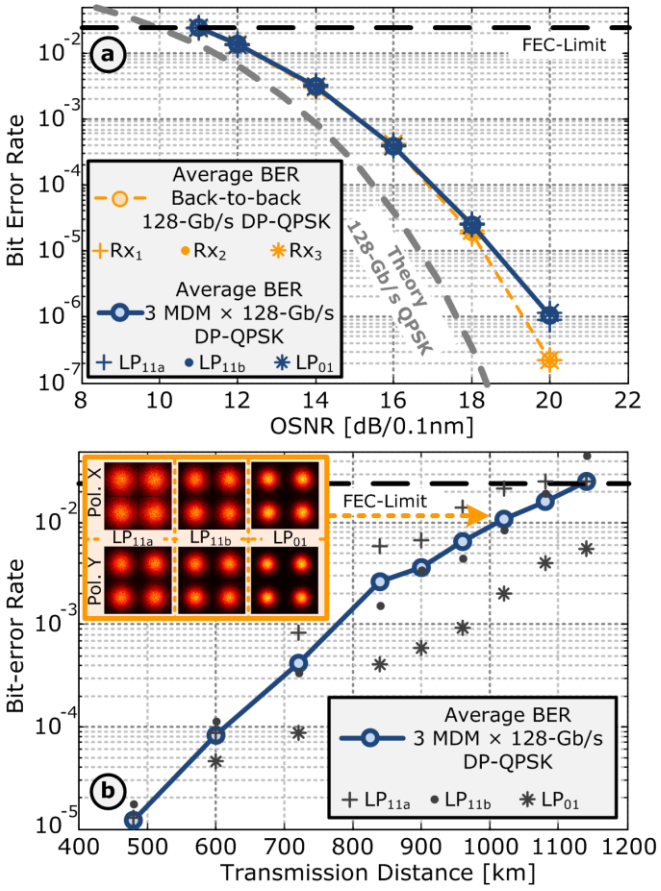

Fig. 5. a) Back-to back performance of the 128-Gb/s DP-QPSK for all three coherent receivers (orange) and 3 MDM × 128-Gb/s DP-QPSK. b) Transmission distance versus bit-error rate for 3 MDM × 128-Gb/s DP-QPSK over the FMF.

At the output of the re-circulating loop a phase-plate based mode de-multiplexer was used to mode de-multiplex the three signals. The 193.4 THz CUT was filtered out using 50 GHz tunable filters and afterwards fed to three coherent receivers connected to two digital sampling scopes: an 8 port 40-Gsamples/s scope (20 GHz electrical bandwidth) and a 4 port 50-Gsamples/s scope (16 GHz electrical bandwidth). Both digital sampling

scopes were carefully synchronized beforehand to assure all signals are received time-aligned. Afterwards, offline 6×6 MIMO-DSP was employed to reconstruct the sent signals [15].

Fig. 5a shows the back-to-back performance of the 128-Gb/s DP-QPSK signal in the single-mode domain for all three coherent receivers (Rx) and when mode multiplexed and de-multiplexed. The performance shows a 1 dB penalty with respect to theory at the FEC-limit, assumed at $2.4 \cdot 10^{-2}$ [17], in the single-mode regime for all Rxs and a very small penalty (<0.1 dB) for MDM.

Fig. 5b shows the transmission distance versus bit-error rate. After 1020 km an average BER over all modes of $\sim 1.1 \cdot 10^{-2}$ is reached, with all modes still performing below the FEC-limit. After 1080 km and 1140 km the BER increased to $1.6 \cdot 10^{-2}$ and $2.6 \cdot 10^{-2}$, respectively, with the $LP_{11}a$-signal performing the worst as a result of the MDL and being above the assumed FEC-limit. The inset shows the recovered constellations after 1020 km.

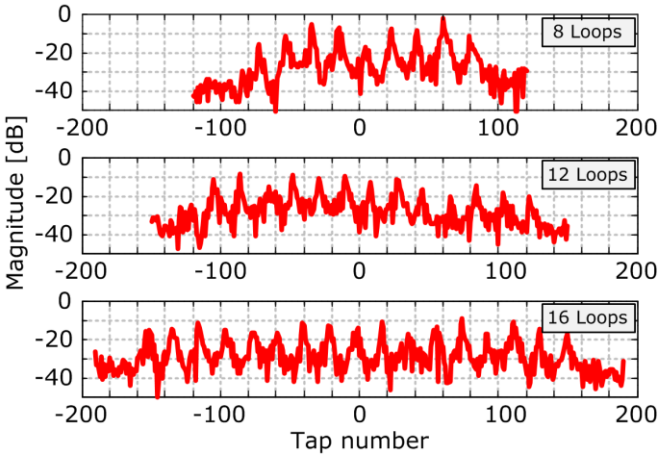

Fig. 6. Impulse response after 8 Loops (480 km), 12 Loops (720 km) and 16 Loops (960 km) of transmission.

Although the modes are separately excited using the phase-plate base mode MUX, during transmission the modes start to mix and 6×6 MIMO-DSP is required to undo the mixing. Fig. 6 shows one the 36 impulse responses obtained after 8 loops (480 km), 12 loops (720 km) and 16 loops (960 km), respectively. After 8 loops 9 peaks are observed, each spaced at ~18 taps apart from each other. This is a result of the 9 symbols DGD between the LP_{01} and LP_{11} modes which occurs each loop, and therefore another peak appears after each loop. This can be observed after 12 loops and 16 loops, having 13 and 17 peaks, respectively, indicating proper performance of the optical chopper based re-circulating loop.

In conclusion, we have presented the basic principles of an optical chopper based re-circulating loop, enabling emulation of long-haul FMF transmission using only a limited amount of fiber. An over 1000 km transmission distance transmission of 3 MDM × 128-Gb/s DP-QPSK was presented using the optical chopper re-circulating loop, showing proper functioning of the loop enabling further research in long-haul FMF transmission.

This work was supported by the EU FP7-ICT MODEGAP project (grant agreement 258033).

We thank Coriant R&D Munich for their support.

References

1. D.G. Foursa, H.G. Batshon, H. Zhang, M. Mazurczyk, J.-X Cai, O. Sinkin, A. Pilipetskii, G. Mohs, and N.S. Bergano, in *Proc. European Conference on Optical Communication (ECOC,2013)*, paper PD3.E.1.
2. M. Salsi, R. Rios-Muller, J. Renaudier, P. Tran, L. Schmalen, A. Ghazisaeidi, H. Mardoyan, P. Brindel, G. Charlet, and S. Bigo, in *Proc. European Conference on Optical Communication (ECOC, 2013)*, paper PD3.E.2.
3. V.A.J.M. Sleiffer, Z. Maalej, D. van den Borne, M. Kuschnerov, V. Veljanovski, M. Hirano, Y. Yamamoto, T. Sasaki, S.L. Jansen, A. Napoli, and H. de Waardt, Opt. Express **19**, B710 (2011).
4. C. Behrens, D. Lavery, D.S. Millar, S. Makovejs, B.C. Thomsen, R.I. Killey, S.J. Savory, and P. Bayvel, in *Proc. European Conference on Optical Communication (ECOC, 2011)*, paper Mo.2.B.2.
5. R.-J. Essiambre, G. Kramer, P.J. Winzer, G.J. Foschini, and B. Goebel, J. Lightw. Technol. **28**, 662 (2010).
6. D. J. Richardson, J.M. Fini, and L.E. Nelson, Nat. Photonics **7**, 354 (2013).
7. R.-J. Essiambre, R. Ryf, N.K. Fontaine, and S. Randel, IEEE Phot. J. **5** (2012).
8. R. Hui, and M. O'Sullivan, in *Fiber Optic Measurement Techniques*, eds. (Elsevier Academic Press, 2009), pp. 481-630.
9. N.S. Bergano, and C.R. Davidson, J. Lightw. Technol. **13**, 879 (1995).
10. S. Randel, R. Ryf, A.H. Gnauck, M.A. Mestre, C. Schmidt, R.-J. Essiambre, P.J. Winzer, R. Delbue, P. Pupalaikis, A. Sureka, Y. Sun, X. Jiang, and R. Lingle, in *Proc. Optical Fiber Communication Conference (OFC, 2012)*, paper PDP5C.5.
11. R. Ryf, S. Randel, N.K. Fontaine, M. Montoliu, E. Burrows, S Chandrasekhar, A.H. Gnauck, C. Xie, R.-J. Essiambre, P.J. Winzer, R. Delbue, P. Pupalaikis, A. Sureka, Y. Sun, L. Grüner-Nielsen, R.V. Jensen, and R. Lingle, in *Proc. Optical Fiber Communication Conference (OFC, 2013)*, paper PDP5A.1.
12. E. Ip, M. Li, Y.-K. Huang, A. Tanaka, E. Mateo, W. Wood, J. Hu, Y. Yano, and K. Koreshkov, in *Proc. Optical Fiber Communication Conference (OFC, 2013)*, paper PDP5A.2.
13. V.A.J.M. Sleiffer, H. Chen, Y. Jung, M. Kuschnerov, D.J. Richardson, S.U. Alam, Y. Sun, L. Grüner-Nielsen, N. Pavarelli, B. Snyder, P. O'Brien, A.D. Ellis, A.M.J. Koonen, and H. de Waardt, in *Proc. IEEE Photonics Conference (IPC, 2013)*, paper PD6.
14. L. Grüner-Nielsen, Y. Sun, J. W. Nicholson, D. Jakobsen, K. G. Jespersen, R. Lingle, and B. Pálsdóttir, J. Lightw. Technol. **30**, 3693 (2012).
15. V.A.J.M. Sleiffer, Y. Jung, N. Baddela, J. Surof, M. Kuschnerov, V. Veljanovski, J. Hayes, N.V. Wheeler, E. Numkam Fokoua, J. Wooler, D. Gray, N. Wong, F. Parmigiani, S.U. Alam, M. Petrovich, F. Poletti, D.J. Richardson, and H. de Waardt, J. Lightw. Technol. **32**, 854 (2014)
16. Y. Jung, Q. Kang, V.A.J.M. Sleiffer, B. Inan, M. Kuschnerov, V. Veljanovski, B. Corbett, R. Winfield, Z. Li, P.S. Teh, A. Dhar, J. Sahu, F. Poletti, S.-U. Alam, and D.J. Richardson, Opt. Express **21**, 10383 (2013).
17. D.A. Morero, M.A. Castrillon, F.A. Ramos, T.A. Goette, O.E. Agazzi, and M.R. Hueda, Global Telecommunications Conference (GLOBECOM 2011).